www.czasopisma.pan.pl PAN POLSKA AKADEMIA NAUK www.journals.pan.pl

A R C H I V E S O F M E T A L L U R G Y A N D M A T E R I A L S

Volume 59 2014 Issue 4

DOI: 10.2478/amm-2014-0221

K. MROCZKA*

CHARACTERISTICS OF AlSi9Mg/2017A ALUMINUM ALLOYS FRICTION STIR WELDED WITH OFFSET WELDING LINE AND ROOT-SIDE HEATING

CHARAKTERYSTYKA STOPÓW ALUMINIUM AlSi9Mg/2017A ZGRZEWANYCH METODĄ FRICTION STIR WELDING Z PRZESUNIĘCIEM LINII ZGRZEWANIA I DODATKOWYM ŹRÓDŁEM CIEPŁA OD STRONY GRANI

Welding of materials differing significantly in terms of chemical composition and microstructure is one of the main advantages of the Friction Stir Welding method. This paper presents the results of welding of a cast AlSi9Mg (hypoeutectic silumin) and 2017A aluminum alloys. The welding was performed with a high linear velocity (over 1 m/min). The modification of the process consisted in offsetting the welding line toward the advancing side, and in on application of an additional heat source from the root side. The study of the macrostructure (with high resolution of the image) revealed the presence of defects in the weld, despite greater plasticity of the material results from raising the temperature. The analysis (by SEM, SEM-EDS) of constituent stable phases within the cast alloy, showed their considerable fragmentation, however to a various degree. The material above the weld nugget was not mixed and contained micro-defects that did not result from the welding. The hardness distribution within the weld nugget, reveals slight strengthening of the both cast and wrought alloys. A metastable state of the 2017A alloy was also documented, however, the alloy hardness increased within the weld nugget due to the natural aging. On the other hand, the hardness of the heat-affected zone in this alloy does not increase also due to the natural aging.

Keywords: FSW, aluminium alloys, AlSi9Mg, 2017A

Jedną z głównych zalet technologii FSW jest zdolność do spajania materiałów znacznie różniących się składem chemicznych. W artykule przedstawiono rezultaty zgrzewania stopów aluminium AlSi9Mg (silumin podeutektyczny) i 2017A. Zgrzewanie wykonano z dużą prędkością liniową (powyżej 1 m/min). Proces zgrzewania zmodyfikowano przesuwając linię zgrzewania w kierunku strony natarcia oraz stosując dodatkowe źródło ciepła od strony grani. Badania makrostruktury zgrzeiny wykazały obecność wad mimo zwiększonej plastyczności materiału podczas zgrzewania, w wyniku podwyższenia temperatury. Podczas zgrzewania FSW dochodzi do fragmentacji cząstek w obszarze działania narzędzia. Na podstawie badań SEM i SEM-EDS wykazano różny stopień fragmentacji wydzieleń w stopie AlSi9Mg. Badania wykazały ponadto ograniczoną intensywność mieszania materiału przez narzędzie w strefie nad jądrem zgrzeiny. W tym obszarze występują również niewielkich rozmiarów wady, niebędące efektem płynięcia materiału. Z kolei analizy rozkładów twardości na przekroju porzecznym zgrzeiny dowiodły niewielkiego umocnienia stopu odlewniczego. Natomiast stop 2017A, w obszarze jądra zgrzeiny, wykazał niestabilność mikrostruktury (bezpośrednio po zgrzewaniu) oraz uległ umocnieniu w wyniku starzenia naturalnego. Starzeniu nie uległ obszar strefy wpływu ciepła.

1. Introduction

Friction Stir Welding (FSW) technology is a solid state welding method [1] and, therefore, a number of disadvantages that occur during fusion welding are not observed in the microstructure [2-4]. Severe plastic deformation and intensive material flow induced by the FSW rotating tool constitute the basis of this method of welding. The advantage of the friction stir welding [5] is a much smaller amount of heat applied to the joint area. This reduces the size of the heat-affected zone. Conventional FSW joining is performed using a tool consisting of a pin and shoulder – the overall shape resembles a screw where the pin is the threaded part and the shoulder is the bolt head. Some of the changes within the FSW tool, for example, the rates of rotation of the pin and shoulder are different, can give good results for structure quality of welds [6]. The FSW method is also applied to structural modification of materials as the Friction Stir Processing (FSP) [7]. However, the greatest advantage of this method consists in joining unweldable materials, for example various composites or precipitation hardened aluminum alloys (e.g. 2000, 7000 series) [1, 5, 8]. Also, it can be used to weld dissimilar materials. Like steel/Al [9] or Al/Cu. This technology may be useful in the search for methods of welding different types of composites with complex matrix and different reinforcement phases [10-13].

The main feature of FSW welds is their typical morphology (lack of symmetry, the presence of thermo-mechanically affected zone (TMAZ) including so-called weld nugget) described in many studies [1, 6, 9, 14]. However, the basic prob-

* INSTITUTE OF TECHNOLOGY, PEDAGOGICAL UNIVERSITY OF CRACOW, 2 PODCHORĄŻYCH STR., 30-084 KRAKÓW, POLAND

lem is a frequently occurring defects (flaws or voids of the material), usually at the bottom of the weld. The main condition for obtaining acceptable quality joint is sufficient plasticity of materials during the welding. Sometimes heat input (generated during welding) could be not enough to achieve the proper flow of the materials. From the technological point of view, welding parameters and/or the shape of the tool [8, 15] could be changed to improve the conditions of the flowing material. However, the conditions of heat transfer from the welded area, especially to the bottom, could also be modified. The material flow under these conditions is highly varied depending on the location within the weld [16, 17].

Because of the ability to obtain dissimilar joints [9], the 2017A and AlSi9Mg joints are used to estimate the impact of parameters, conditions and additional heat input on the microstructure and properties of the FSW joint. The first of the materials (2017A) is a wrought one, the other is a cast alloy – hypoeutectic silumin. The parameters that have been chosen to perform the experiment provide a good quality face of the weld, but inside, at the advancing side, there are defects of considerable size – when welding is currying out along the line of materials contact. The offsetting of the welding line considerably improves the quality of the microstructure but does not completely eliminate the discontinuity (flaws) in the microstructure. The results of these experiments are discussed in more detail in Ref. [6]. Raising the temperature from the weld side, along the direction of the greatest heat loss, is expected to result in increasing in the plasticity of the material and improving its ability to flow and, consequently, improve the quality of the weld. Such solutions are described in the literature [19], but they are based only on the reduction of the thermal conductivity of the backing plate on which the welding is performed. The current experiment involves heating of the materials from the root side.

Besides the description of the microstructure and properties of the weld, the aim was also to determine the size of particles present in the particular weld areas, especially on the AlSi9Mg side.

2. Experimental method

2017A-T451 and AlSi9Mg aluminum alloys in the form of sheet and cast plate, respectively, with the thickness of 6 mm were used in this experiment. The chemical composition of the alloys is presented in Table 1. Butt welds were made parallel to the rolling direction of the alloy 2017A sheet. The welding process was performed with a conventional FSW tool: a pin with the diameter of 8 mm, a shoulder with the diameter of 22 mm, the angle between the tool shoulder and the surface of welded sheets was 1.5°.

In relation to the edges of the welded elements, the welding line was offset about 1.5 mm toward the alloy 2017A. Additional heat source was applied – the root side of the welded elements was heated by two heaters, placed along the welding line placed (Fig. 1). The temperature of 100°C was achieved before the launch of welding. TMP (temperature measurement point) in Fig. 1 is also presented. Parameters of the welding and were: the rate of rotation of 560 rpm, linear velocity of 1120 mm/min and 1.5 mm shifting the FSW tool (the welding line) toward to 2017A aluminum alloy.

TABLE 1
Chemical composition of 2017A and AlSi9Mg aluminum alloys (wt.%)

Alloy	Cu	Mg	Mn	Si	Zn	Fe	Al
2017A	4.14	0.72	0.6	0.68	0.18	0.31	bal.
AlSi9Mg	0.21	0.31	0.34	8.6	0.14	0.64	bal.

The samples were investigated after natural aging (three weeks after welding). The studies of the mechanical properties were carried out to determine hardness profiles μHV0.1 at cross-sections. Measurements were taken at distances of 1 and 3 mm from the surface of the weld (face of weld).

Scanning electron microscopy (SEM) – the JEOL 6610LV equipped with an energy dispersive X-ray spectrometer (EDS) manufactured by Oxford EDS detector controlled by AZtec software – was used to investigate the surface of samples (sections). The surface was polished mechanically before SEM examination.

The microstructure investigations were conducted using the OLYMPUS GX51 light microscope with Nomarski differential interference contrast optics and Stream-Motion software. The light-microscopic observations were performed on surfaces that were polished mechanically and then etched with a solution containing 2 ml HF, 4 ml HNO_3 and 94 ml H_2O. Macrostructure image of joint section was created on the basis of microscopic images (magnification x50). 30 to 40 images were composed into macrostructure applying the Image Composite Editor (ICE) software [18]. The quantitative metallography analysis of the particles of AlSi9Mg alloy was conducted on the basis of light microscope micrographs, without etching, observed at x500 magnification. The particles area and shape factors were calculated using SigmaScanPro5 and Excel Microsoft software.

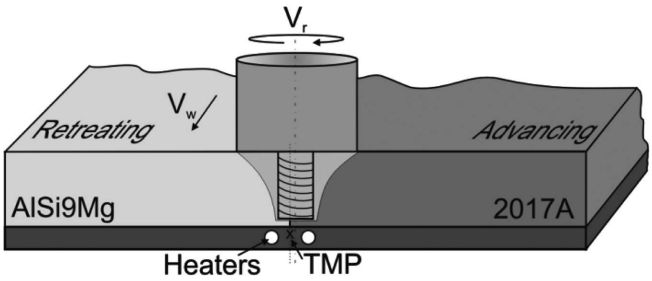

Fig. 1. The schema of the welding process with additional heat source; TMP – Temperature Measurement Point

3. Results

Figure 2 shows the macrostructure of the weld produced with the offset welding line and with an additional source of heat (as in Fig. 1). This observation helped to estimate the macro-structural distribution of the alloys in the weld and possible defects location. The Figure 2 also shows boundaries of areas where the pattern of precipitations clearly indicates

different directions of the material flow (marked by dotted lines). The welding defects were formed along directions of the material flow – Fig. 3.

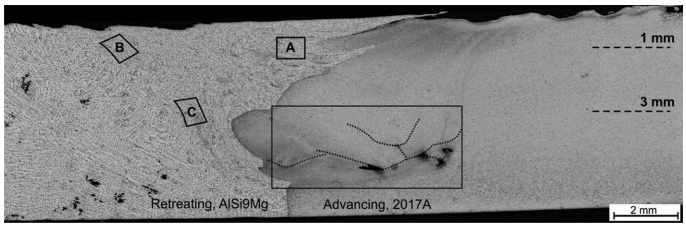

Fig. 2. Macrostructure of cross-section of the weld

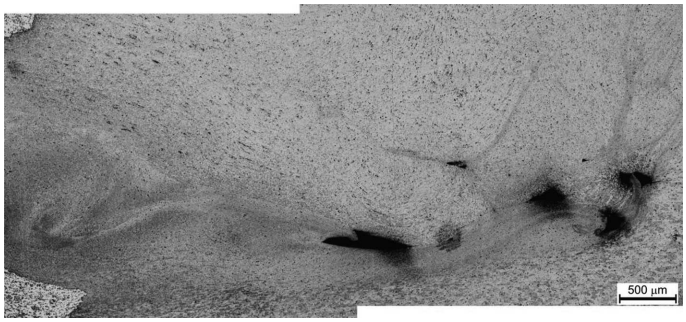

Fig. 3. Microstructure of cross-section of the weld – defects at the bottom of weld nugget, advancing side; the magnificated area marked by the rectangle in Fig. 2

Detailed studies of the microstructure were performed for the selected locations in the weld, indicated in Fig. 2 (A, B, C letters – areas about 0.3 mm^2). The study was aimed at determination of the particle size present in the AlSi9Mg alloy. The results are shown in Table 2, and in the form of histograms – Fig. 4 and Fig. 5.

TABLE 2

Analysis of particles in the AlSi9Mg alloy within the weld and the parent material – A, B and C locations marked in Fig. 2

Average	Place in Fig. 2			Parent material
	A	B	C	
Area [μm^2]	7.88	14.40	9.84	87.04
Shape Factor	0.592	0.596	0.601	0.482

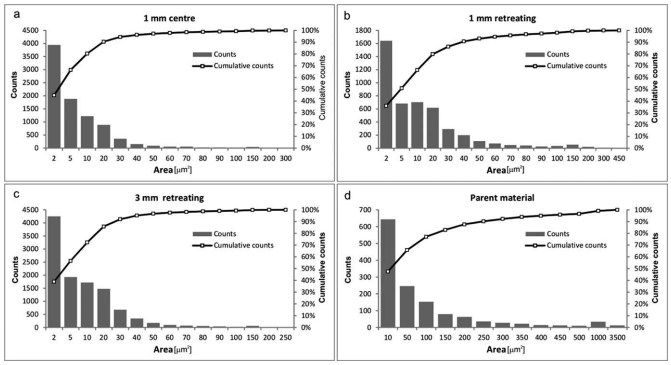

Fig. 4. Histograms – particles area measurements for places in Fig. 2: a) A – 1 mm in the centre, b) B – 1 mm at the retreating side, c) C – 3 mm at the retreating side, d) parent material

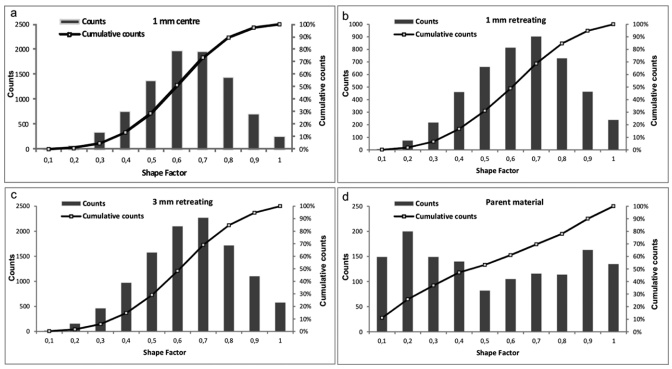

Fig. 5. Histograms – particles Shape Factor measurements for places in Fig. 2: a) A – 1 mm in the centre, b) B – 1 mm at the retreating side, c) C – 3 mm at the retreating side, d) parent material

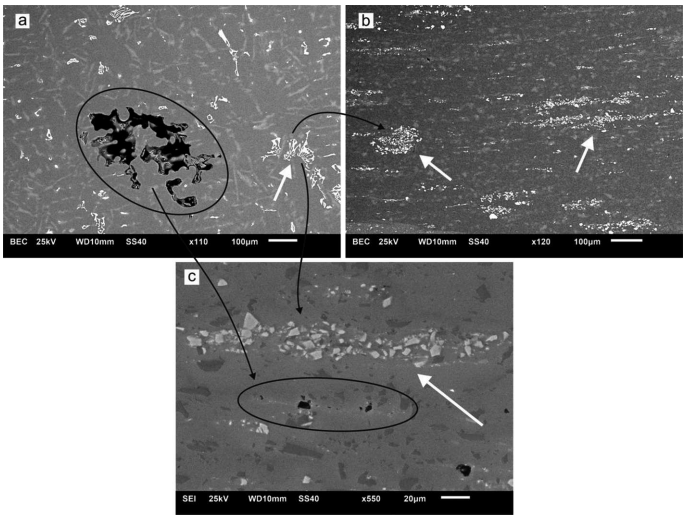

Fig. 6. SEM microstructure of cross-section: a) AlSi9Mg parent material, b) and c) areas between the weld nugget and the weld face

The microstructure of the parent material and a weld area between the weld nugget and the weld face were also examined by SEM. The results are presented in Fig. 6. The system of bands and aggregations containing particles was observed. These areas are indicated by white arrows in Fig. 6b and Fig. 6c. Chemical composition measurement of these particles revealed presence of Al, Fe, Mn, Si. Phases of the same chemical composition also occur in the parent material (Fig. 6a, white arrow indication), where casting defects, like shrinkage defects, are observed as well. It is also presented in encircled areas in Fig. 6a and 6c. Small, micrometers flaws of the microstructure are also visible near the bands mentioned above – Fig. 6c. Black arrows in Fig. 6 indicate relationship between particular areas within parent material and within the joint – vanishing of defects and the fragmentation of constituent phases.

Figure 7 shows hardness distribution of the area including: the heat affected zone (on both sides of the joint) and the weld nugget, 3 mm from the face weld. The position of the measurement line on the cross section is also shown in Fig. 2 as a dashed line. The Figure also shows the results of the parent materials hardness measurements (both alloys). The results are shown in relation to the welding line and the place of contact plates before welding.

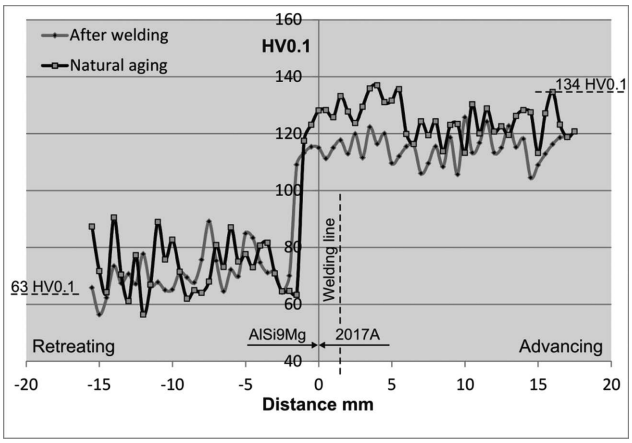

Fig. 7. Hardness distribution on the cross section of the weld – 3 mm from face of the weld; dashed line indicates the welding line (FSW tool position relative to the edge of the welded elements)

4. Discussion

4.1. Macrostructure, defects

The critical point in the weld, where defects are the most likely found, is the area located near the bottom of the weld, mainly at the advancing side. Simultaneously, it is the region penetrated by the tool pin, i.e. the border of the FSW tool's workplace. The location of the defects is shown in Fig. 2, while their details are presented in Fig. 3. The defects are formed in the border of areas where the material flowed in different directions that was proved due to an analysis of the pattern of precipitates. The largest defects (located at the bottom – Fig. 3) are directly in the end of the pin's workplace. The material located below was not mixed by the FSW tool and flowed to a limited extent as a result of the material's viscosity, while the material above was directly deformed plastically by the pin tool. In the regions where the friction between the flowing streams of material was large enough, the connection (joint) was created and complete metallurgical continuity of material was observed there. According to various sources [20], the temperature of this material in the pin workplace's area can be in the range from about 400°C to more than 530°C, while in the heat affected zone, about 240°C at the advancing, and 190°C at the retreating side [20], without using any additional heat sources. Therefore, the use of the additional heat source should lead to an increase of the temperature at the pin workplace and at the place where the defects are forming. This increase may reach several dozens of degrees (C°). As shown above, the rise of the temperature does not cause a sufficient increase of the material's plasticity to fill the voids forming by the movement of the FSW tool during the flow of the material. The comparison of the microstructure quality with the quality weld of produced with the same parameters and welding conditions, but without additional heating, leads to the conclusion that no expected results were obtained – the weld quality deteriorated.

4.2. Microstructure and particles analysis

Analysis of the microstructure of the tested joint and other aluminum welds performed using the conventional FSW (i.e. without modification, such as a different pin and shoulder rotation speed [6]) showed significant differences in the microstructure of the weld nugget and in the area above it. In this case, this variation is also due to the independent participation both of materials in the weld – the weld nugget is made of the 2017A alloy, which results from the fact that this alloy is located at the advancing side. On the other hand, the area between the nugget and the crown side of the weld contains the AlSi9Mg alloy. The AlSi9Mg alloy participation in the joint made it possible to determine the range of mixing of material and the degree of microstructure fragmentation. This analysis was based on measurements of particles present in the alloy. The particles could be accurately distinguished from the matrix using the images of the light microscope. These measurements were related to the size of particles and their shape factor. The eutectic Si particles and the particles containing of Al, Fe, Mn, Si were subjected to analysis. The analysis of the chemical composition was performed using the SEM-EDS method. The precipitates results from the contamination of the alloy by these elements. This phase was not identified during this study, however, the literature [21] informs, that $Al_{15}(FeMn)_3Si$ phase commonly exist within commercial cast alloys. The mentioned phase was fragmented in the same way as eutectic silicon due to similar brittleness (relative to the plastic matrix). In addition, both phases were formed under similar conditions, as primary phases, i.e. from the liquid state. This means that they are stable to the eutectic temperature. Moreover, in the case of the phase containing Fe, even above this temperature. The stability of these particles to the eutectic temperature (577°C, according to the equilibrium phase Al-Si) brings about the constant volume fraction of these phases during friction stir welding. The FSW takes place in the solid state [1] and at lower temperature then 577°C, as mentioned earlier.

Quantitative analyses were performed for selected areas in the weld, indicated by the letters A, B, C in Fig. 2, The largest fragmentation of precipitates is observed in the center of the weld (area A). This area is mainly deformed by the tool shoulder. Furthermore, significant fragmentation also occurs in the middle part of the retreating side of the weld, 3 mm from the face – area C. The material is deformed there only by the tool pin. On the other hand, the lowest fragmentation is revealed for the area nearby the face of the weld (1 mm – area B), also at the retreating side, where the material is deformed only by the tool shoulder. The difference between values for the area (B) and for the weld center (area A), (the same distance from the face) is quite significant, about 45%. Regardless of the place within the weld, the particle fragmentation is very high in comparison to the parent material. The average particle size is up to 11 times greater. As far as the results of particle size, measurements are concerned the calculation of the shape factor (SF) bring to interesting conclusions. Variations in the value (for individual areas – Table 1) are negligibly small (up to 0.009) for all particles within the weld. This suggests that the particles breaking have a brittle character. The particles break perpendicular to the long side. Although the particle size is significantly different, the shape is similar. The value of the SF (about 0.6) corresponds to the shape of a polyhedron (value 1 – is typical for a sphere [22]). On the other hand, the result for the parent material

clearly prove that precipitates within this material are strongly elongated. However, it should be noted that the analysis was carried out on the basis of two-dimensional observation, while the tested phases within the material have three-dimensional and more complex shapes. Such shapes result from the kinetics the crystallization within liquid matrix of the alloy.

4.3. The upper part of the weld microstructure

Observations of the microstructure details of the area above the weld nugget show heterogeneity in the form of bands and aggregations (Fig. 6b and Fig. 6c). The phases that create these clusters (bands and aggregations) were discussed above. These phases exist in parent material in the form of skeletal shape, as is presented in Fig. 6a and indicated by white arrow. The operation of the FSW tool has not produced the uniform distribution of particles within the weld. Instead, the clusters of particles were only formed, as is indicated by arrows in Fig. 6a, Fig. 6b and Fig. 6c. This observation surprisingly suggests that the material in the area above ??the weld nugget is sufficiently plastically deformed to make fragmentation of the phases but the material is not stirred by the FSW tool. The examined area also contains a number of small, micrometer defects (voids). An example of that is presented in Fig. 6c, encircled area. Their presence, in turn, can be associated with the material shrinkage in the parent alloy. This defects resulted from shrinkage may occur in (gravity) cast components [23, 24, 28]. An example of such a defect is shown in Fig. 6a, and encircled by the ellipse. It can be assumed that when the defect of a sufficiently large size is in the welding area (on top), it will not be completely closed (healed) as a result of plastic deformation. It means that the degree of plastic deformation in this area is limited. It is also partly due to the lack of material mixing in this area. Similar results were also obtained in the welds between the same AlSi9Mg alloy.

4.4. Mechanical properties – hardness distributions

The studies of mechanical properties of the weld were evaluated by hardness measurements performed on a weld cross-section. Determination of hardness distributions is one of the most common methods of studying mechanical properties of FSW joints noted in the literature [5, 15, 17]. At the retreating side, the diversity of hardness is quite significant, ranging from 56 to 90 HV0.1. – Fig. 7. This is a result of the microstructure of AlSi9Mg alloy, which consists of a relatively soft matrix (aluminum solid solution) and contains a significant amount of particles, mainly the Si phase. It is typical state of not heat treated cast hypoeutectic silumin. The results of hardness measurements of this type of microstructure, as well as composites reinforced with particles, are subjected to considerable scatter of results.

The average hardness of the area are equal to 71 and 73HV0.1, for the sample in the as-welded state and after natural aging, respectively. The results show that the material does not undergo natural aging to a significant extent. There was, however, the strengthening of the material as a result of FSW because the average hardness of the parent material is 63HV0.1 – Fig. 7. The strengthening can be explained by changes in the alloy matrix – the refinement of grains, which, according to the Hall-Petch rule, leads to an increase in the yield strength (point) of a metallic material. This matter has been discussed by Yutaka S. Sato et al. [25] regarding aluminum and 5083 aluminum alloy processed with the FSW tool. 2017A aluminum alloy is in the area of the weld nugget and at the advancing side; it hardened by precipitation, mainly by phases containing Cu (GP, Θ',Θ", Al_2CuMg [26]). Throughout the weld (in the as-welded state) at the 2017A alloy side, a decrease in hardness compared to the average hardness of the parent material was found (134 HV0.1 – Fig. 7). In the area of the weld nugget, where the material was the most intensely deformed and stirred, the strengthening occurs because of natural aging. It reaches hardness values close to the hardness of the parent material. However, in the heat affected zone, the hardness increase is much smaller, but noticeable – the material (the zone) does not reach the average hardness of the base material. The increase in hardness in the (artificial and natural) aging processes is the effect of precipitates formation preventing dislocation movements. It can be therefore assumed that the center of the weld was supersaturated by elements coming from dissolved phases. Thus, hardness decrease "after welding" and afterwards again creation of precipitates (aging) resulted in the strengthening of the weld. The exposition to higher temperature (up to about 530°C) is very short (approx. 1 s – the tool is moved by a distance equal to its diameter, i.e. 8 mm). There will be no saturation of the matrix in such a short time under static conditions even at the temperature of 530°C (this is acceptable supersaturation temperature of 2017A alloy [27]). However, the dissolution process of strengthening particles, in this case, is strongly supported by the dynamic, multi-directional and large plastic deformation. Components of dissolving particles are able to quickly diffuse within the crystal structure where a large number of different types of defects are present. Mechanical mixing (stirring) of the material will also be supported by the dissolution of the particles. Furthermore, it can be assumed that under the conditions of plastic deformation induced by the FSW tool (in particular the pin) micro-areas may appear where the temperature is much higher than the experimentally determined 530°C. Though, this theory was not justified by experiments and regular studies. The hardness decrease because of welding and its increase as a result of ageing was well documented. It is well known that precipitation hardening results from supersaturation state of a material matrix and further ageing. The range of supersaturation of the alloys in different places within a weld, types of precipitates and kinetics of their formation will be further studied.

5. Conclusions

The scope of the experiments and research can be summarized in the following conclusions:

1. The use of additional heat source has not produced expected results – defects are still present inside the weld in the form of cavities that are formed at the borders of the streams of the flowing material. Defects were found in the lower part of the pin workplace, at the advancing side.
2. The friction stir welding caused fragmentation of phases within AlSi9Mg alloy. The average particles area was significantly reduced from 87 μm^2 (for parent material)

to about 8 to 14 μm^2 within the weld, depending on the location. However, the particles different in size exhibited very similar shape.

3. The material is not mixed (stirred) in the area between the weld nugget and the face (crown side). The heterogeneity of this area is mainly due to the existence of local bands containing particles. The microstructure is a result of the material flowing in one direction. The degree of plastic deformation in this area is so large that it causes fragmentation of phases, however, is too small to remove (close) the casting defects, produce by shrinkage.
4. The AlSi9Mg cast alloy hardness slightly increases as a result of the welding process. However, the alloy is not strengthened by natural aging. The effect of welding on 2017A alloy is more significant. The material in the heat-affected zone is weakened, while partial supersaturation was observed in the weld nugget; afterwards, it is strengthened as a result of natural aging. This means that the part of the weld immediately after welding, is in a metastable state.

Acknowledgements

Partial financing of this research by Ministry of Science and Higher Education, Poland, Research Grant N N508 618940 is acknowledged.

FSW process was done in the Institute of Welding in Gliwice, Poland by Dr. Eng. Adam Pietras.

Instrumentation co-financed by the European Regional Development Fund under the Infrastructure and Environment Programme, for the Development of the Infrastructure and Environment.

REFERENCES

[1] C. Yeni, S. Sayer, O. Ertuğrul, M. Pakdil, Effect of post-weld aging on the mechanical and microstructural properties of friction stir welded aluminum alloy 7075, Archives of Materials Science and Engineering **34**(2), 105-109 (2008).

[2] A. Kula, L. Blaz, M. Sugamata, Microstructure and mechanical properties of rapidly solidified Al-Fe-Ni-Mg alloys, Materials Science Forum **674**, 165-170 (2011).

[3] A. Kula, L. Blaz, M. Sugamata, Structural and mechanical features of rapidly solidified Al-2Fe-Ni-5Mg alloy, Solid State Phenomenon **186**, 279-282 (2012).

[4] E. Fras, E. Olejnik, Interaction between solidification front and alien phase particles, Archives of Metallurgy and Materials **53**(3), 695-702 (2008).

[5] F. Rui-dong, S. Zeng-qiang, S. Rui-cheng, L. Ying, L. Hui-jie, L. Lei, Improvement of weld temperature distribution and mechanical properties of 7050 aluminum alloy butt joints by submerged friction stir welding, Materials and Design **32**, 4825-4831 (2011).

[6] K. Mroczka, A. Pietras, Characteristics of dissimilar Friction Stir Welded joints of selected aluminum alloys, Conference proceedings: Joining of Advanced and Specialty Material, Material Science and Technology 2012, Pittsburgh, Pennsylvania USA, 308-315 (2012).

[7] M. St. Węglowski, A. Pietras, Friction Stir Processing – analysis of the process. Archives of Metallurgy and Materials **56**(3), 779-788 (2011).

[8] M. St. Węglowski, A. Pietras, A. Węglowska, Effect of welding parameters on mechanical and microstructural properties of Al 2024 joints produced by friction stir welding, Journal of Kones Powertrain and Transport **19**, 523-532 (2009).

[9] H. Uzun, C.D. Donne, A. Argagnotto, T. Ghidini, C. Gabaro, Friction stir welding of dissimilar Al 6013-T4 to X5CrNi18-10 stainless steel, Materials and Design **26**, 41-46 (2005).

[10] A. Kula, L. Blaz, M. Sugamata, J. Kaneko, Effect of annealing temperature on the structure and mechanical properties of mechanically alloyed AlMg – Nb_2O_5 and AlMg – $ZrSi_2$ composites, Journal of Microscopy **237**, 421-426 (2010).

[11] A. Janas, A. Kolbus, E. Olejnik, On the character of matrix-reinforcing particle phase boundaries in MeC and MeB (Me = W, Zr, Ti, Nb, Ta) in situ composites, Archives of Metallurgy and Materials **54**(2), 319-327 (2009).

[12] P. Kurtyka, N. Ryłko, Structure analysis of the modified cast metal matrix composites by use of the RVE theory, Archives of Metallurgy and Materials **58**(2), 357-360 (2013).

[13] E. Fraś, A. Janas, P. Kurtyka, S. Wierzbiński, Structure and properties of cast Ni_3Al/TiC and Ni_3Al/TiB_2 composites. PART I. SHSB Method applied in fabrication of composites based on intermetallic phase Ni_3Al reinforced with particles of TiC and TiB_2. Archives of Metallurgy **48**(4), 383-408 (2003).

[14] D. Shusheng, Y. Xinqi, L. Guohong, J. Bo, Comparative study on fatigue properties between AA2024-T4 friction stir welds and base material, Materials Science and Engineering A **435-436**, 389-395 (2006).

[15] W. Yuan, R.S. Mishra, S. Webb, Y.L. Chen, B. Carlson, D.R. Herling, G.J. Grant, Effect of tool design and process parameters on properties of Al alloy 6016 friction stir spot welds, Journal of Materials Processing Technology **211**, 972-977 (2011).

[16] M. St. Węglowski, S. Dymek, Microstructural modification of cast aluminium alloy AlSi9Mg via Friction Modified Processing, Archives of Metallurgy and Materials **57**, 71-78 (2012).

[17] P. Bala Srinivasan, K.S. Arora, W. Dietzel, S. Pandey, M.K. Schaper, Characterisation of microstructure, mechanical properties and corrosion behaviour of an AA2219 friction stir weldment, Journal of Alloys and Compounds **492**, 631-637 (2010).

[18] A. Wójcicka, Z. Wróbel, The panoramic visualization of metallic materials in macro- and microstructure of surface analysis using Microsoft Image Composite Editor (ICE), Lecture Notes in Computer Science **7339**, 358-368 (2012).

[19] P. Upadhyay, A.P. Reynolds, Effect of backing plate thermal property on friction stir welding of 25 mm thick AA6061, Conference proceedings: 9^{th} Friction Stir Welding Symposium, Huntsville, Alabama USA, 2012, CD-session 3A.

[20] J. Adamowski, C. Gambaro, E. Lertora, M. Ponte, M. Szkodo, Analysis of FSW welds made of aluminium alloy AW6082-T6, Archives of Materials Science and Engineering **28**(8), 453-460 (2007).

[21] G. Mrówka-Nowotnik, J. Sieniawski, M. Wierzbińska, Intermetallic phase particles in 6082 aluminium alloy, Archives of Materials Science and Engineering **28**(2), 69-76 (2007).

[22] SigmaScanPro5, User's Guide, 2004.

[23] W.W. Bose-Filho, E.R. de Freitas, V.F. da Silva, M.T. Milan, D. Spineli, Al-Si cast alloys under isothermal and thermomechanical fatigue conditions, International Journal of Fatigue **29**, 1846-1854 (2007).

[24] M. H a j j a r i, E. D i v a n d a r i, An investigation on the microstructure and tensile properties of direct squeeze cast and gravity die cast 2024 wrought Al alloy, Materials and Design **29**, 1685-1689 (2008).

[25] Y.S. S a t o, M. U r a t a, H. K o k a w a, K. I k e d a, Hall/Petch relationship in friction stir welds of equal channel angular-pressed aluminium alloys, Materials Science and Engineering **354**, 298-305 (2003).

[26] C. G e n e v o i s, D. F a b r e g u e, A. D e s c h a m p s, W.J. P o o l e, On the coupling between precipitation and plastic deformation in relation with friction stir welding of AA2024 T3 aluminium alloy, Materials Science and Engineering A **441**, 39-48 (2006).

[27] K. M r o c z k a, A. W ó j c i c k a, P. K u r t y k a, 2017A aluminum alloy in different heat treatment conditions, Acta Metallurgica Slovaca **18**(2-3), 82-91 (2012).

[28] B. R a m s, A. P i e t r a s, K. M r o c z k a, Friction Stir Welding made of elements made of cast aluminium alloy, Archives of Metallurgy and Materials 59, 1 (2014) DOI: 10.2478/amm-2014-0064.

Received: 20 January 2014.